Published in final edited form as:
Free Radic Biol Med. 2012 June 1; 52(0): 2312–2319. doi:10.1016/j.freeradbiomed.2012.04.011.

Obesity-induced tissue free radical generation: An *in vivo* immuno-spin trapping study

Nicholas K.H. Khoo[a], **Nadiezhda Cantu-Medellin**[b,c], **Jason E. Devlin**[d], **Claudette M. St. Croix**[d], **Simon C. Watkins**[d], **Alexander M. Fleming**[b], **Hunter C. Champion**[c], **Ronald P. Mason**[e], **Bruce A. Freeman**[a], and **Eric E. Kelley**[a,b,c,*]

[a]Department of Pharmacology and Chemical Biology, University of Pittsburgh, School of Medicine, Pittsburgh, PA 15213, USA

[b]Department of Anesthesiology, University of Pittsburgh, School of Medicine, Pittsburgh, PA 15213, USA

[c]Vascular Medicine Institute, University of Pittsburgh, School of Medicine, Pittsburgh, PA 15213, USA

[d]Center for Biological Imaging, University of Pittsburgh, School of Medicine, Pittsburgh, PA 15213, USA

[e]Laboratory of Pharmacology and Toxicology, National Institute of Environmental Health Science, Research Triangle Park, NC 27709, USA

Abstract

Assessment of tissue free radical production is routinely accomplished by measuring secondary by-products of redox reactions and/or diminution of key antioxidants such as reduced thiols. However, immuno-spin trapping, a newly developed immunohistochemical technique for detection of free radical formation, is garnering considerable interest as it allows for the visualization of 5, 5-dimethyl-1-pyrroline *N*-oxide (DMPO)-adducted molecules. Yet, to date, immuno-spin trapping reports have utilized *in vivo* models in which successful detection of free radical adducts required exposure to lethal levels of oxidative stress not reflective of chronic inflammatory disease. To study the extents and anatomic locations of more clinically relevant levels of radical formation, we examined tissues from high-fat (HF) diet-fed mice, a model of low-grade chronic inflammation known to demonstrate enhanced rates of reactive species production. Mice subjected to 20 weeks of HF diet displayed increased free radical formation (anti-DMPO mean fluorescence staining) in skeletal muscle (0.863 ± 0.06 units vs 0.512 ± 0.07 units), kidney (0.076 ± 0.0036 vs 0.043 ± 0.0025), and liver (0.275 ± 0.012 vs 0.135 ± 0.014) compared to control mice fed normal laboratory chow (NC). Western blot analysis of tissue homogenates confirmed these results showing enhanced DMPO immunoreactivity in HF mice compared to NC samples. The obesity-related results were confirmed in a rat model of pulmonary hypertension and right heart failure in which intense immunodetectable radical formation was observed in the lung and right ventricle of monocrotaline-treated rats compared to saline-treated controls. Combined, these data affirm the utility of immuno-spin trapping as a tool for *in vivo* assessment of altered extents of macromolecule oxidation to radical intermediates under chronic inflammatory conditions.

*Corresponding author at: University of Pittsburgh, School of Medicine, Departments of Anesthesiology and Pharmacology, W-1357 Biomedical Sciences Tower, 200 Lothrop Street, Pittsburgh, PA 15213, United States. Fax: +1 412 648 9587. ekelley@pitt.edu(E.E. Kelley).

Keywords

Free radicals; Immuno-spin trapping; Obesity; Inflammation; Oxidative stress

Introduction

Inflammatory-linked pathologies affect an exponentially growing population of individuals in the developed world and are strongly associated with an increased incidence of obesity. A consequence of obesity-induced metabolic disorders in both animal models and clinically is an increased rate of production of reactive inflammatory mediators resulting from the hypoxic and hyperglycemic environment found in vessels and tissues [1]. Obesity-induced elevation in oxidant and free radical formation is attributable to altered mitochondrial electron transport, NADPH oxidase activation, glucose autoxidation, uncoupled endothelial nitric oxide synthase, reactions of advanced glycation end-products, and enhanced xanthine oxidoreductase activity [1–3]. These reactive species propagate tissue dysfunction and further inflammatory responses, promoting the incidence of adverse obesity-related clinical responses [3]. More incisive understanding regarding the timing of onset, extent, and anatomic localization of tissue free radical generation would facilitate the design of mechanistically targeted treatment strategies to combat this disease.

Assessment of enhanced rates of free radical formation in tissues is routinely accomplished by measuring the accumulation of more stable secondary by-products of redox reactions and/or diminution of small-molecule antioxidants such as glutathione. However, there are significant limitations associated with these methods including: (1) the inability to identify anatomic sites of production because of the necessity of homogenizing or freezing and then sectioning samples before addition of probes, (2) the promiscuous reactions of indicator molecules that lead to ambiguous identification of the chemical identity of the instigating species, and (3) redox-cycling of the indicator molecule leading to artificial amplification of the signal [4]. Taken together, these issues affirm the need for novel techniques to more precisely examine oxidant and free radical formation in living tissues.

Combining the reactivity of the electron paramagnetic resonance (EPR)[1] spin trap 5, 5-dimethyl-1-pyrroline *N*-oxide (DMPO) with free radicals and a polyclonal antibody toward a DMPOoctanoic acid conjugate, immuno-spin trapping allows for the visualization of DMPO-adducted molecules [5]. This approach capitalizes on two chemical characteristics of DMPO: (1) the rate constant for DMPO with carbon radicals (C•) and most other free radicals is ~10^7 M^{-1} s^{-1}, making DMPO competitive with O_2 ($K_{oxygen/C\bullet}$ = ~ 10^9 M^{-1} s^{-1}), especially in inflamed tissues where O_2 concentrations are significantly diminished, and (2) the covalent bond formed between DMPO and carbon-centered and other radicals captures DMPO in the tissue, thus making it available for binding with the anti-DMPO antibody (Fig. 1) [5, 6]. Immuno-spin trapping has identified specific molecular sites of radical formation in purified preparations of protein and DNA as well as indicating overall levels of radical formation in cell lysates and rodents exposed to a lethal oxidative insult immediately before sacrifice, such as exposure of liver tissue to acetone or injections of high-dose lipopolysaccharide [6–10]. We evaluated DMPO immuno-spin trapping for the capacity to detect tissue free radical formation occurring under chronic low-grade inflammatory conditions comparable to events experienced clinically by subjecting mice to either a HF or a NC diet. We confirmed these observations in an alternative model of chronic systemic inflammation, monocrotaline-induced pulmonary hypertension.

Materials and methods

Materials

Anti-DMPO polyclonal antibody (ALX-210–530-R050) was purchased from Enzo Life Sciences (Farmingdale, NY, USA). DMPO was from Dojindo (Japan). Monocrotaline was from Sigma– Aldrich (St. Louis, MO, USA).

Mouse feeding protocol

C57BL/J6 male mice were purchased from The Jackson Laboratory (Bar Harbor, ME, USA). The high-fat (HF) diet was purchased from Research Diets (D12492; New Brunswick, NJ, USA). Obesity was induced by HF diet feeding (with 60% of the adjusted calories derived from fat) for 20 weeks beginning at age 6–8 weeks. Age-matched controls were maintained on a standard rodent chow diet (15% adjusted calories derived from fat; Pro Lab RHM 3000 rodent diet; PMI Feeds, St. Louis, MO, USA). Mice were fed ad libitum for 20 weeks and given free access to water. All rodent studies were conducted under the approval of the University of Pittsburgh Institutional Animal Care and Use Committee (Protocol No. 1009934 and 0909554).

Mouse DMPO protocol

After 20 weeks of either HF (60% calories derived from fat) or NC diet, mice received DMPO dissolved in pyrogen-free saline ip (1.5 g/kg total) in three doses 18, 12, and 6 h before sacrifice as previously [6]. At sacrifice, organs/tissues were perfused with phosphate-buffered saline (PBS; pH 7.4), removed, and (a) fixed for immunohistochemical analysis (see below) or (b) frozen in liquid N2 and stored at −80 °C for Western blot analysis.

Rat monocrotaline protocol

Male Sprague–Dawley rats (200–250 g) were randomly divided into control and monocrotaline-treated groups. Rats received a single subcutaneous injection of 60 mg/kg monocrotaline or normal saline (0.9% NaCl). After 4 weeks, the rats were injected with DMPO dissolved in pyrogen-free saline ip (2 g/kg total) in three doses 18, 12, and 6 h before sacrifice. Tissues were harvested and treated before immunohistochemical analysis as described below.

Immunohistochemistry

Lungs were inflated and tissues/organs were fixed in 2% paraformaldehyde in PBS (pH 7.4). After fixation, tissues/organs were removed and placed in 30% sucrose for 24 h and then frozen using 2-methyl butane and liquid N_2. Tissues were then sectioned (7 μm), placed in PBS, and permeabilized with 0.1% Triton X-100 for 20 min. After being blocked with 2% bovine serum albumin in PBS, the samples were stained for DMPO–protein adduct formation using polyclonal anti-DMPO and Alexa Fluor 488 anti-rabbit IgG. Nonspecific fluorescence was assessed by applying only the secondary antibody. Slices were mounted on microscope cover glasses (22 × 22 × 1.5 mm) and sections analyzed by confocal microscope (Olympus). Quantification of mean fluorescence intensity (MFI) per nucleus per field was accomplished by converting all images to grayscale followed by analysis with Scion Image software.

Western blot

The detection of DMPO–protein adducts was determined as previously [6]. Briefly, tissues were homogenized in Chelex-treated PBS (pH 7.4) + diethylenetriaminepentaacetic acid (100 μM) and then centrifuged at 3000 rpm at 4 °C for 20 min to remove insoluble materials. Samples were reduced and denatured by treatment with tris(2-

carboxyethyl)phosphine (TCEP; 0.5 mM) for 5 min at 70 °C. It is important to note that dithiothreitol may induce dissociation of DMPO from target biomolecules, hence the rationale for using TCEP as a reducing agent. After SDS–PAGE of 20 mg protein/lane and transfer to polyvinylidene difluoride membranes, DMPO-adducted proteins were assessed using rabbit anti-DMPO (1:1000, v/v) followed by a goat anti-rabbit IgG (1:5000, v/v; Upstate Biotechnologies). Blots were developed using ECL-Plus chemiluminescence (GE/Amersham). Protein concentrations were determined using the Pierce BCA assay. Band intensity was assessed using UScanIt software.

Statistics

Data were analyzed using one-way analysis of variance followed by Tukey's range test for multiple pair-wise comparisons. Significance was determined as $p < 0.05$.

Results

After 20 weeks of HF or NC diet, the immunodetection of DMPO reaction was observed on the periphery of muscle fibers of the gastrocnemius (Fig. 2). Mice placed on a HF diet demonstrated a greater degree of MFI/nucleus (0.863 ± 0.06 units) than NC mice (0.512 ± 0.07 units; $p < 0.05$, $n = 6$; Fig. 2B). Tissue sections from HF mice that did not receive DMPO and those not treated with primary antibody did not display significant fluorescence increases. Similar results were obtained from the parallel Western blot analysis of gastrocnemius homogenates prepared from HF and NC samples (Fig. 2C). Densitometric analysis of the total staining for the entire lane revealed a 1.87-fold greater intensity in the gastrocnemius of HF mice compared to NC (7.1 ± 0.4 HF vs 3.8 ± 0.51 NC, $p < 0.05$, $n = 3$; Fig. 2D).

Greater tissue DMPO reactivity was also revealed by immunofluorescence of liver tissue from HF mice (0.27 ± 70.012 units) compared to NC-fed mice (0.135 ± 0.014 units; $p < 0.05$, $n = 6$; Fig. 3A and B). The presence of DMPO adducts was prominent around central venules and portal areas in the sections from HF mice, but absent from the NC samples. Neither HF mice that did not receive DMPO nor NC tissue sections not treated with primary antibody displayed significant tissue fluorescence. These results were confirmed by Western blots of liver homogenates prepared from HF and NC samples (Fig. 3C). Densitometric analysis of total staining for the entire lane revealed a 1.7-fold higher intensity in the HF samples compared to NC (33.9 ± 2.4 units HF vs 19.95 ± 3.1 units NC, $p < 0.05$, $n=3$; Fig. 3D).

Examination of renal tissue also exposed a greater presence of DMPO-adducted molecules in the HF samples compared to NC (Fig. 4). The HF diet-induced enhancement of DMPO immunoreactivity appears within the simple cuboidal epithelial layer as well as adjacent to the basement membrane of the renal tubules. The fluorescence intensity for the HF samples (0.076 ± 0.0036 units) was substantially greater than for NC mice (0.043 ± 0.0025 units; Fig. 4B). The immunohistochemical results were again consistent with Western blots of kidney homogenates in which the total staining of the respective lanes revealed significantly greater immunodetectable protein (16.2 ± 0.8 units HF vs 13.3 ± 0.3 units NC, $p < 0.05$, $n = 3$) in HF compared to NC (Figs. 4C and 4D).

This method was confirmed in a well-established *in vivo* model of oxidative inflammatory tissue injury: a single injection of monocrotaline (MCT) that ultimately leads to pulmonary arterial hypertension [11]. Four weeks after receiving MCT or saline (sham), rats were sacrificed and both the lung and the right ventricle were sectioned and stained for DMPO-adducted macromolecules. MCT-treated rats exhibited pronounced DMPO reactivity in a cross section of the right ventricle, compared to sham-treated controls, in which the

immunofluorescence linked with DMPO reaction was not detectable (Fig. 5, top). Lung parenchymal tissue from MCT-treated rats also displayed significant staining for DMPO compared to sham-treated rats, indicating a considerable increase in tissue free radical production (Fig. 5, bottom).

Discussion

The biological investigation of free radical and redox reactions has relied heavily on measuring secondary reaction by-products of reduced versus oxidized small-molecule antioxidants and scavengers as evidence of free radical production in tissues. Notably, these methods possess shortcomings that limit their capacity to report the extents and anatomic sites of radical formation. Attempts to overcome these limitations by *ex vivo* evaluation of oxidant formation from previously frozen tissue sections with various fluorescent probes are obviously problematic, as freeze–thaw induces loss of membrane integrity with resultant mobilization of redox-active metals as well as loss of compartmentalization of key substrates driving the enzymatic formation of reactive species. Recently, these shortcomings are becoming more incisively addressed via the use and detection of more specific biochemical probes for free radical and oxidative reaction products [12, 13]. For example, sites of tissue oxidant generation can be indicated by the formation of hydroethidine (HE) oxidation products; however, multiple fluorescent products are formed independent of reaction with $O_2^{\bullet -}$ [14]. As such, it is unclear to what extent the reported signal is dependent upon the fluorescence of the $O_2^{\bullet -}$-specific HE oxidation product (2-OH-E^+). Although some advances have been made to bridge the gap between these techniques and those that afford the visualization of free radical production *in situ* there exists a need for improvement. Immuno-spin trapping is a strong candidate for bridging this gap as it allows for the visualization of anatomic sites of tissue radical formation as well as the relative amount being produced. However, similar to all other methods for radical and oxidant detection, immuno-spin trapping has limitations. For example, immuno-spin trapping cannot determine the source or the identity of the oxidant responsible for initiating the formation of DMPO-reactive unpaired electrons on biomolecules. Likewise, quantitation of radical formation by immuno-spin trapping is limited to the extent of staining intensity and as such the technique is best characterized as a barometer of overall oxidative stress. However, when used in combination with alternative methods, immuno-spin trapping may be used to significantly augment our understanding of oxidant formation and allied contributions to disease processes.

A key question pertaining to immuno-spin trapping is sensitivity. Specifically, it remains unclear if this technique possesses the sensitivity necessary to detect differences in tissue radical formation under conditions where levels of oxidative stress are more reflective of those seen clinically during chronic inflammation. This is exemplified by the very limited comprehensive *in vivo* evaluation of immuno-spin trapping for which reports utilized lethal levels of oxidant stressors to successfully detect tissue radical formation or have shown analysis of a single tissue under sublethal oxidative stress conditions [6, 9, 15–17]. Therefore, we chose to test the capacity of immuno-spin trapping to detect tissue radical formation induced by obesity-related chronic inflammation. We chose this model and these tissues as it has been reported, using alternative methods, that HF diet-induced obesity leads to increased levels of ROS-related products in the plasma, skeletal muscle, liver, and kidney [18–21]. For example, subjecting male C57BL/6J mice to a HF diet for 16 weeks induced increased levels of protein carbonyls and TBARS in the plasma as well as in the gastrocnemius muscle [22]. Therefore, we assumed that if immuno-spin trapping can be used to detect these nonlethal obesity-induced inflammatory-mediated increases in ROS-driven free radical formation, then it would be a significant advancement in the arsenal of tools available to assess oxidative stress *in vivo*.

When mice were exposed to 20 weeks of a HF diet, treatment with DMPO revealed significantly elevated levels of DMPO staining in the gastrocnemius, liver, and kidney compared to those maintained on NC (Figs. 2–4). It is important to note that our DMPO dose (1.5 g/kg) was chosen using previous reports as a template [6, 9] because pharmacokinetic data are not yet available. Our logic for such a relatively high dose is rooted in the concept that DMPO must compete with other reactants including molecular oxygen for free radicals formed by enhanced oxidative stress in the tissue. Hence, higher levels of DMPO enhance the probability of generating covalently DMPO-adducted biomolecules resulting in antigenic targets for immunohistochemistry. We conducted pilot experiments to ensure the absence of demonstrable side effects at this dosage and delivery schedule. Western blot analysis of tissue homogenates confirmed an increased presence of DMPO-adducted proteins in HF mice. Whereas Western blotting results clearly show greater DMPO staining in the HF lanes (Figs. 2C, 3C, and 4C), there were subtle differences in changes in signal intensity between HF and NC compared to immunohistochemical image analysis. This may be a consequence of samples used for Western blotting that were homogenized, fractionated free of insoluble proteins, and then denatured for electrophoretic separation. As such, compared to tissue sections, there may be different extents of antigen (DMPO) presentation for antibody recognition. Importantly, the clear definition of DMPOadducted proteins on Western blots revealed that mass spectrometry- based proteomic analysis can be applied to detect specific protein radicals that adduct to DMPO. Taken together, these results suggest immuno-spin trapping is a useful tool for exploring free radical formation in obesity models of chronic oxidative stress.

To confirm the specificity of this approach for obesity-induced tissue macromolecule free radical generation in an alternative model of chronic inflammation/oxidative stress, rats were injected with MCT [11, 23]. This induced vascular remodeling, proliferation of smooth muscle cells, endothelial dysfunction, inflammatory cytokines, and oxidative stress resulting in right ventricular remodeling, hypertrophy and pulmonary hypertension [23, 24]. Previous studies have shown that MCT increases markers of oxidative stress in plasma, heart, and lung. MCT-treated rats displayed pronounced increases in right ventricular tissue DMPO staining as opposed to saline-treated shams (Fig. 5, top). These images also reveal extensive remodeling in the right ventricle consistent with previous reports [11, 23, 24]. Likewise, lung tissue of MCT-treated rats expresses considerably elevated DMPO staining compared to saline-treated rats (Fig. 5, bottom), consistent with previous reports of increased oxidant generation in MCT-induced pulmonary hypertension [24].

We have demonstrated the utility of immuno-spin trapping for the *in vivo* detection of enhanced free radical formation induced by chronic inflammation in two rodent models. Both of these models are relevant to clinical issues, as obesity is not only epidemic in the United States but also associated with systemic and pulmonary hypertension as well as increased cardiovascular risk [25]. As such, this new tool for the assessment of extents and sites of tissue free radical production is a useful caliper for the redox toolbox.

Acknowledgments

This work was funded by the American Heart Association, a National Scientist Development grant (E.E.K.), R01-HL058115, R01-HL64937, P01-HL103455 (B.A.F.), and the Gilead Sciences Research Scholars Program in Pulmonary Arterial Hypertension (N.K.H.K.).

Abbreviations

DMPO 5, 5-dimethyl-1-pyrroline *N*-oxide

EPR	electron paramagnetic resonance
HF	high fat
MCT	monocrotaline
MFI	mean fluorescence intensity
NC	normal chow
ROS	reactive oxygen species

References

1. Whaley-Connell A, McCullough PA, Sowers JR. The role of oxidative stress in the metabolic syndrome. Rev. Cardiovasc. Med. 2011; 12:21–29. [PubMed: 21546885]
2. Furukawa S, Fujita T, Shimabukuro M, Iwaki M, Yamada Y, Nakajima Y, Nakayama O, Makishima M, Matsuda M, Shimomura I. Increased oxidative stress in obesity and its impact on metabolic syndrome. J. Clin. Invest. 2004; 114:1752–1761. [PubMed: 15599400]
3. Keaney JF Jr, Larson MG, Vasan RS, Wilson PW, Lipinska I, Corey D, Massaro JM, Sutherland P, Vita JA, Benjamin EJ. Obesity and systemic oxidative stress: clinical correlates of oxidative stress in the Framingham Study. Arterioscler. Thromb. Vasc. Biol. 2003; 23:434–439. [PubMed: 12615693]
4. Tarpey MM, Wink DA, Grisham MB. Methods for detection of reactive metabolites of oxygen and nitrogen: in vitro and *in vivo* considerations. Am. J. Physiol. Regul. Integr. Comp. Physiol. 2004; 286:R431–R444. [PubMed: 14761864]
5. Mason RP. Using anti-5,5-dimethyl-1-pyrroline *N*-oxide (anti-DMPO) to detect protein radicals in time and space with immuno-spin trapping. Free Radic. Biol. Med. 2004; 36:1214–1223. [PubMed: 15110386]
6. Chatterjee S, Ehrenshaft M, Bhattacharjee S, Deterding LJ, Bonini MG, Corbett J, Kadiiska MB, Tomer KB, Mason RP. Immuno-spin trapping of a post-translational carboxypeptidase B1 radical formed by a dual role of xanthine oxidase and endothelial nitric oxide synthase in acute septic mice. Free Radic. Biol. Med. 2009; 46:454–461. [PubMed: 19049863]
7. Kojima C, Ramirez DC, Tokar EJ, Himeno S, Drobna Z, Styblo M, Mason RP, Waalkes MP. Requirement of arsenic biomethylation for oxidative DNA damage. J. Natl. Cancer Inst. 2009; 101:1670–1681. [PubMed: 19933942]
8. Siraki AG, Deterding LJ, Bonini MG, Jiang J, Ehrenshaft M, Tomer KB, Mason RP. Procainamide, but not N-acetylprocainamide, induces protein free radical formation on myeloperoxidase: a potential mechanism of agranulocytosis. Chem. Res. Toxicol. 2008; 21:1143–1153. [PubMed: 18489081]
9. Stadler K, Bonini MG, Dallas S, Duma D, Mason RP, Kadiiska MB. Direct evidence of iNOS-mediated *in vivo* free radical production and protein oxidation in acetone-induced ketosis. Am. J. Physiol. Endocrinol. Metab. 2008; 295:E456–E462. [PubMed: 18559982]
10. Narwaley M, Michail K, Arvadia P, Siraki AG. Drug-induced protein free radical formation is attenuated by unsaturated fatty acids by scavenging drug-derived phenyl radical metabolites. Chem. Res. Toxicol. 2011; 24:1031–1039. [PubMed: 21671642]
11. Zaiman AL, Podowski, M.;Medicherla S, Gordy K, Xu F, Zhen L, Shimoda LA, Neptune E, Higgins L, Murphy A, Chakravarty S, Protter A, Sehgal PB, Champion RM, Tuder RM. Role of the TGF-b/Alk5 signaling pathway in monocrotaline-induced pulmonary hypertension. Am. J. Respir. Crit. Care Med. 2008; 177:896–905. [PubMed: 18202349]
12. Zielonka J, Zielonka M, Sikora A, Adamus J, Joseph J, Hardy M, Ouari O, Dranka BP, Kalyanaraman B. Global profiling of reactive oxygen and nitrogen species in biological systems: high-throughput real-time analyses. J. Biol. Chem. 2012; 287:2984–2995. [PubMed: 22139901]
13. Kalyanaraman B, Darley-Usmar V, Davies KJ, Dennery PA, Forman HJ, Grisham MB, Mann GE, Moore K, Roberts LJ 2nd, Ischiropoulos H. Measuring reactive oxygen and nitrogen species with

fluorescent probes: challenges and limitations. Free Radic. Biol. Med. 2012; 52:1–6. [PubMed: 22027063]

14. Zielonka J, Kalyanaraman B. Hydroethidine- and MitoSOX-derived red fluorescence is not a reliable indicator of intracellular superoxide formation: another inconvenient truth. Free Radic. Biol. Med. 2010; 48:983–1001. [PubMed: 20116425]
15. Ruggiero C, Ehrenshaft M, Cleland E, Stadler K. High-fat diet induces an initial adaptation of mitochondrial bioenergetics in the kidney despite evident oxidative stress and mitochondrial ROS production. Am. J. Physiol. Endocrinol. Metab. 2011; 300:E1047–E1058. [PubMed: 21386058]
16. Cassina P, Cassina A, Pehar M, Castellanos R, Gandelman M, de León A, Robinson KM, Mason RP, Beckman JS, Barbeito L, Radi R. Mitochondrial dysfunction in SOD1G93A-bearing astrocytes promotes motor neuron degeneration: prevention by mitochondrial-targeted antioxidants. J. Neurosci. 2008; 28:4115–4122. [PubMed: 18417691]
17. Barbeito AG, Garringer HJ, Baraibar MA, Gao X, Arredondo M, Núñez MT, Smith MA, Ghetti B, Vidal R. Abnormal iron metabolism and oxidative stress in mice expressing a mutant form of the ferritin light polypeptide gene. J. Neurochem. 2009; 109:1067–1078. [PubMed: 19519778]
18. Odermatt A. The Western-style diet: a major risk factor for impaired kidney function and chronic kidney disease. Am. J. Physiol. Renal Physiol. 2011; 301:F919–F931. [PubMed: 21880837]
19. Noeman SA, Hamooda HE, Baalash AA. Biochemical study of oxidative stress markers in the liver, kidney and heart of high fat diet induced obesity in rats. Diabetol. Metab. Syndr. 2011; 3:17. [PubMed: 21812977]
20. Tomino Y, Hagiwara S, Gohda T. AGE–RAGE interaction and oxidative stress in obesity-related renal dysfunction. Kidney Int. 2011; 80:133–135. [PubMed: 21720304]
21. Lefort N, Glancy B, Bowen B, Willis WT, Bailowitz Z, De Filippis EA, Brophy C, Meyer C, Hojlund K, Yi Z, Mandarino LJ. Increased reactive oxygen species production and lower abundance of complex I subunits and carnitine palmitoyltransferase 1B protein despite normal mitochondrial respiration in insulin-resistant human skeletal muscle. Diabetes. 2010; 59:2444–2452. [PubMed: 20682693]
22. Bonnard C, Durand A, Peyrol S, Chanseaume E, Chauvin MA, Morio B, Vidal H, Rieusset J. Mitochondrial dysfunction results from oxidative stress in the skeletal muscle of diet-induced insulin-resistant mice. J. Clin. Invest. 2008; 118:789–800. [PubMed: 18188455]
23. Schultze AE, Roth RA. Chronic pulmonary hypertension—the monocrotaline model and involvement of the hemostatic system. J. Toxicol. Environ. Health B Crit. Rev. 1998; 1:271–346. [PubMed: 9776954]
24. Redout EM, van der Toorn A, Zuidwijk MJ, van de Kolk CW, van Echteld CJ, Musters RJ, van Hardeveld C, Paulus WJ, Simonides WS. Antioxidant treatment attenuates pulmonary arterial hypertension-induced heart failure. Am. J. Physiol. Heart Circ. Physiol. 2010; 298:H1038–H1047. [PubMed: 20061549]
25. National Center for Health Statistics, NCHS Data Brief No. 56, March 2011. Atlanta: U.S. Department of Health and Human Services, Centers for Disease Control and Prevention;

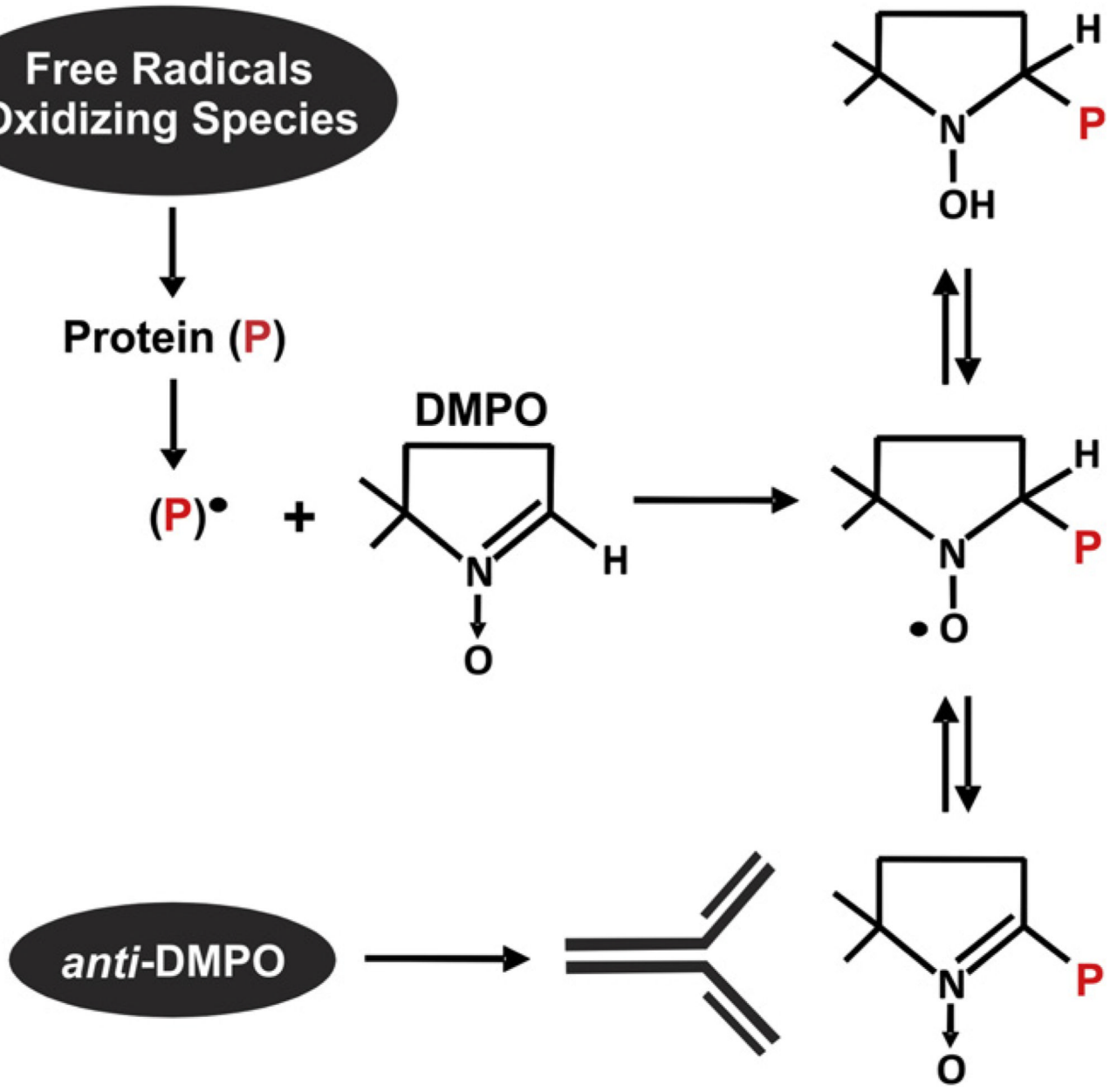

Fig. 1.

Immuno-spin trapping technique. Immuno-spin trapping, a combination of EPR spin trapping and immunohistochemistry, is a recently developed technique for visualizing free radical formation. Using the EPR spin trap 5, 5-dimethyl-1-pyrroline *N*-oxide (DMPO) and a commercially available polyclonal antibody raised to a DMPO–octanoic acid conjugate, free radical formation on biomolecules can be detected. Free radicals on biomolecules covalently adduct to DMPO, effectively sequestering the spin trap and thus making it readily available for antibody detection. This reaction between free radicals on oxidized proteins is greater than 5 orders of magnitude faster than the reaction of superoxide $\left(O_2^{\bullet -}\right)$ with DMPO ($K_{\text{DMPO–superoxide}}$= ~ 3.0 M^{-1} s^{-1} vs $K_{\text{DMPO-biomolecular radicals}}$= ~ 10^7 M^{-1} s^{-1}) [5].

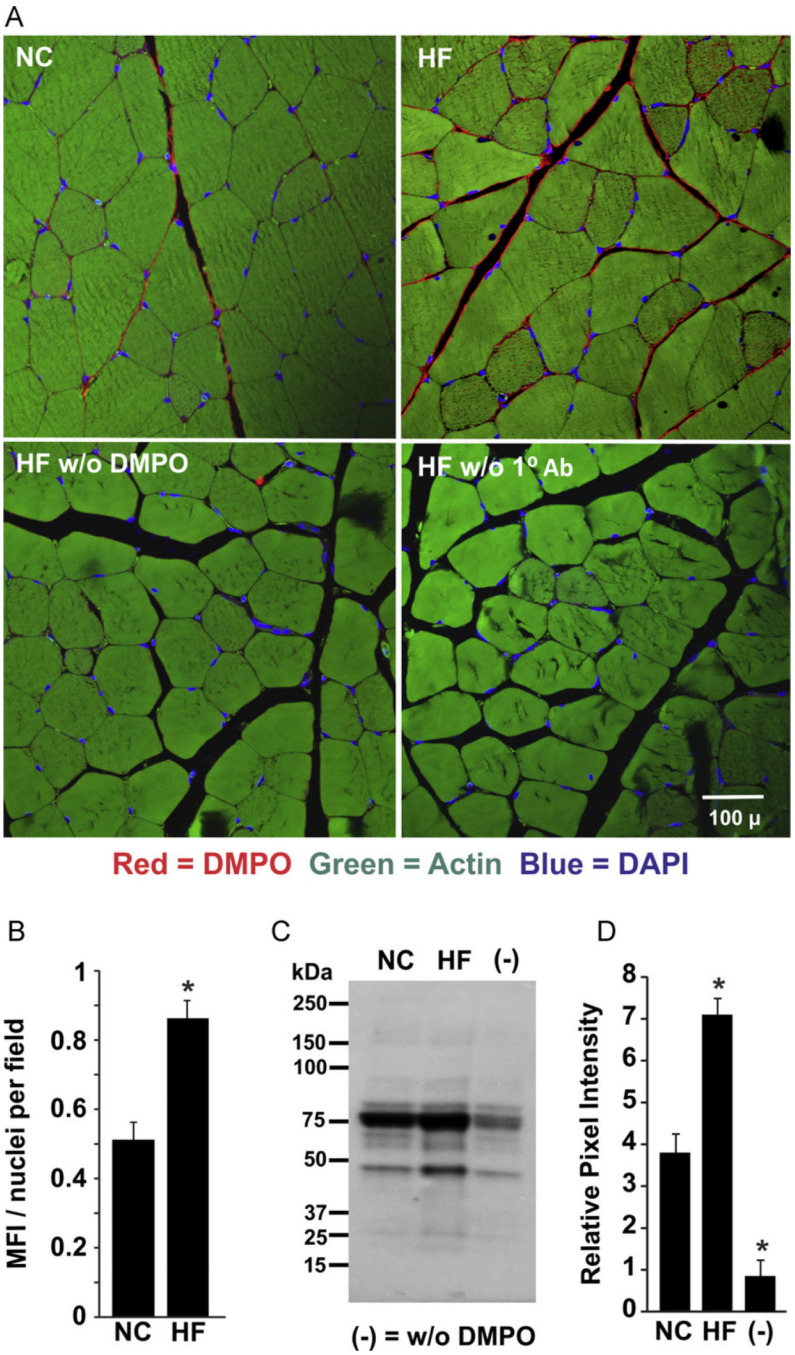

Fig. 2.

Obesity-induced free radical formation in skeletal muscle. (A) After 20 weeks of high-fat (HF) or normal chow (NC) diet, mice received DMPO (1.5 g/kg total ip) in three doses 24, 12, and 6 h before sacrifice or normal saline. At sacrifice, tissue was harvested, fixed, sectioned, and stained for DMPO–protein radicals using a rabbit polyclonal anti-DMPO primary Ab. (B) Mean fluorescence intensity (MFI) and nuclei/field were quantified using MetaMorph software as MFI/nucleus/field for all obesity images. Background from saline-treated mice was subtracted from both NC and HF images. (C) Representative Western blot of gastrocnemius tissues from HF and NC mice. (D) Densitometric analysis of independent

blots using total staining for the entire lane. $p < 0.05$ vs NC (n=6). For (C) and (D), (−) indicates tissue from age-matched normal chow mice injected with 0.9% NaCl.

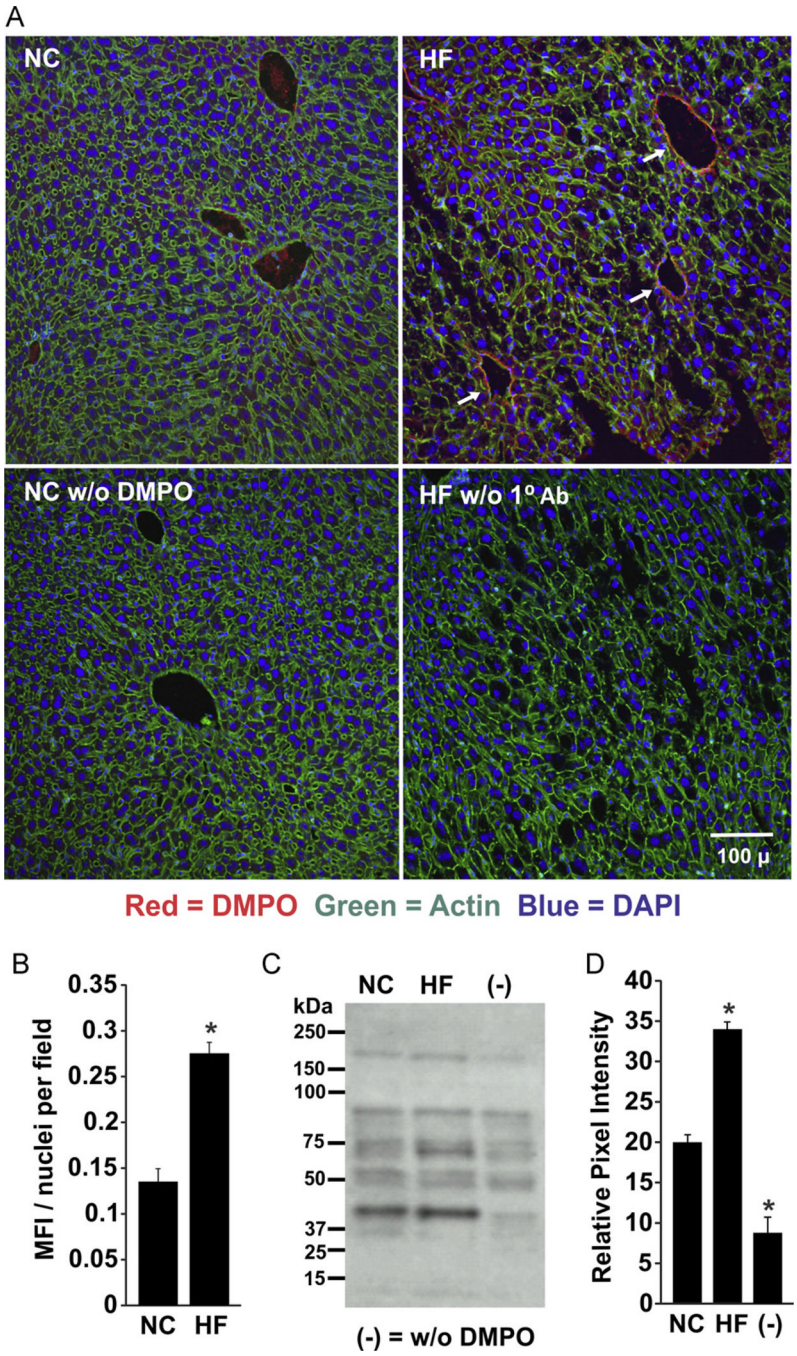

Fig. 3.

Increased free radical formation in hepatic tissue of obese mice. (A) Mice were treated as for Fig. 2 and liver tissue was stained for DMPO–protein radicals using a primary rabbit polyclonal anti-DMPO Ab. (B) MFI and nuclei/field were quantified using MetaMorph software and background from saline-treated mice was subtracted from both NC and HF images. (C) Representative Western blot of liver tissues from HF and NC mice. (D) Densitometric analysis of independent blots using total staining for the entire lane. *$p < 0.05$ vs NC (n=6). For (C) and (D), (−) indicates tissue from age-matched normal chow mice injected with 0.9% NaCl.

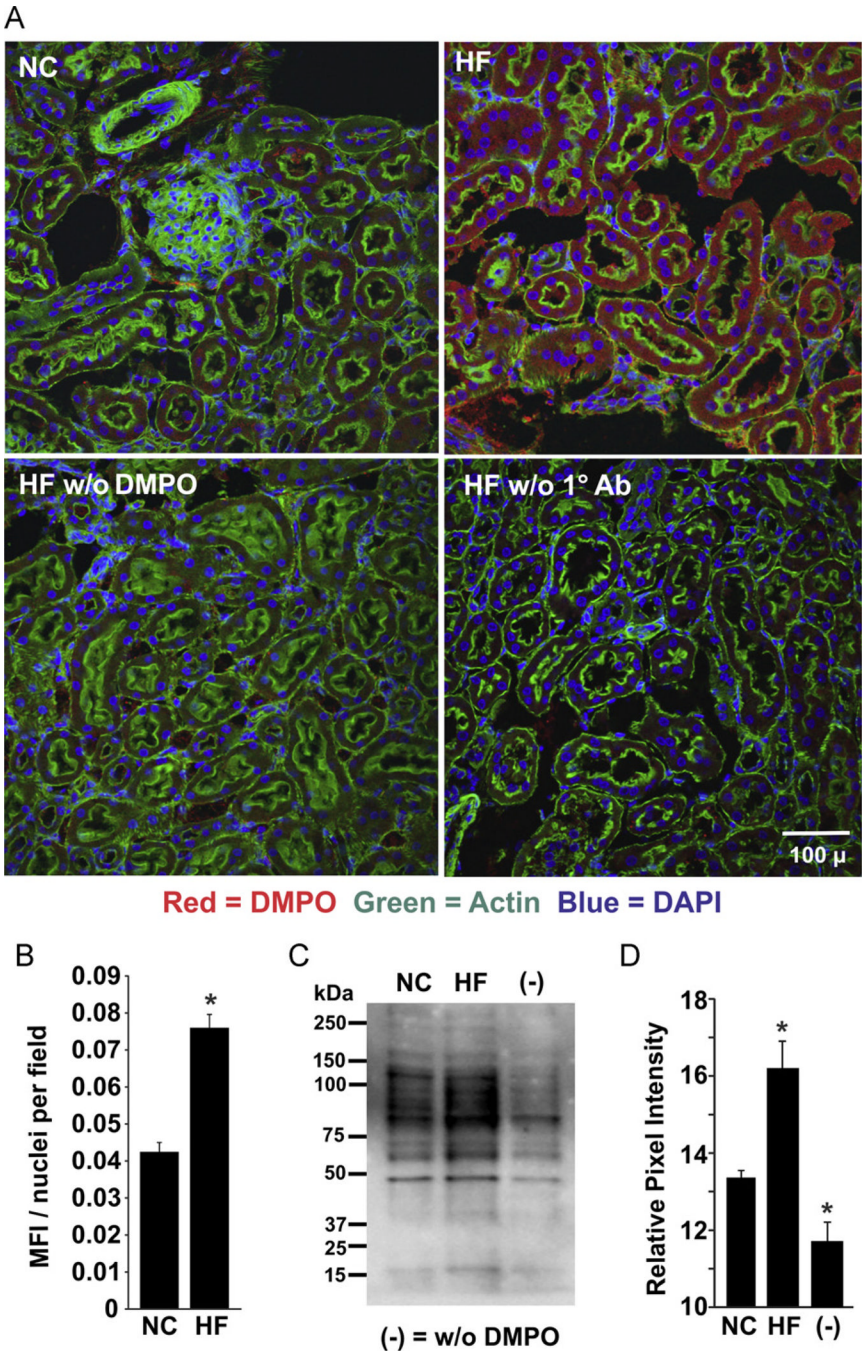

Fig. 4.

Obesity-induced free radical formation in the kidney. (A) Mice were treated as for Fig. 2 and kidney tissue was stained for DMPO–protein radicals using a primary rabbit polyclonal anti-DMPO Ab. (B) MFI and nuclei/field were quantified using MetaMorph software, and background from saline-treated mice was subtracted from both NC and HF images (*$p <$ 0.05 for n=6). (C) Representative Western blot of renal tissues from HF and NC mice. (D) Densitometric analysis of independent blots using total staining for the entire lane. *$p < 0.05$ vs NC (n=6). For (C) and (D), (−) indicates tissue from age-matched normal chow mice injected with 0.9% NaCl.

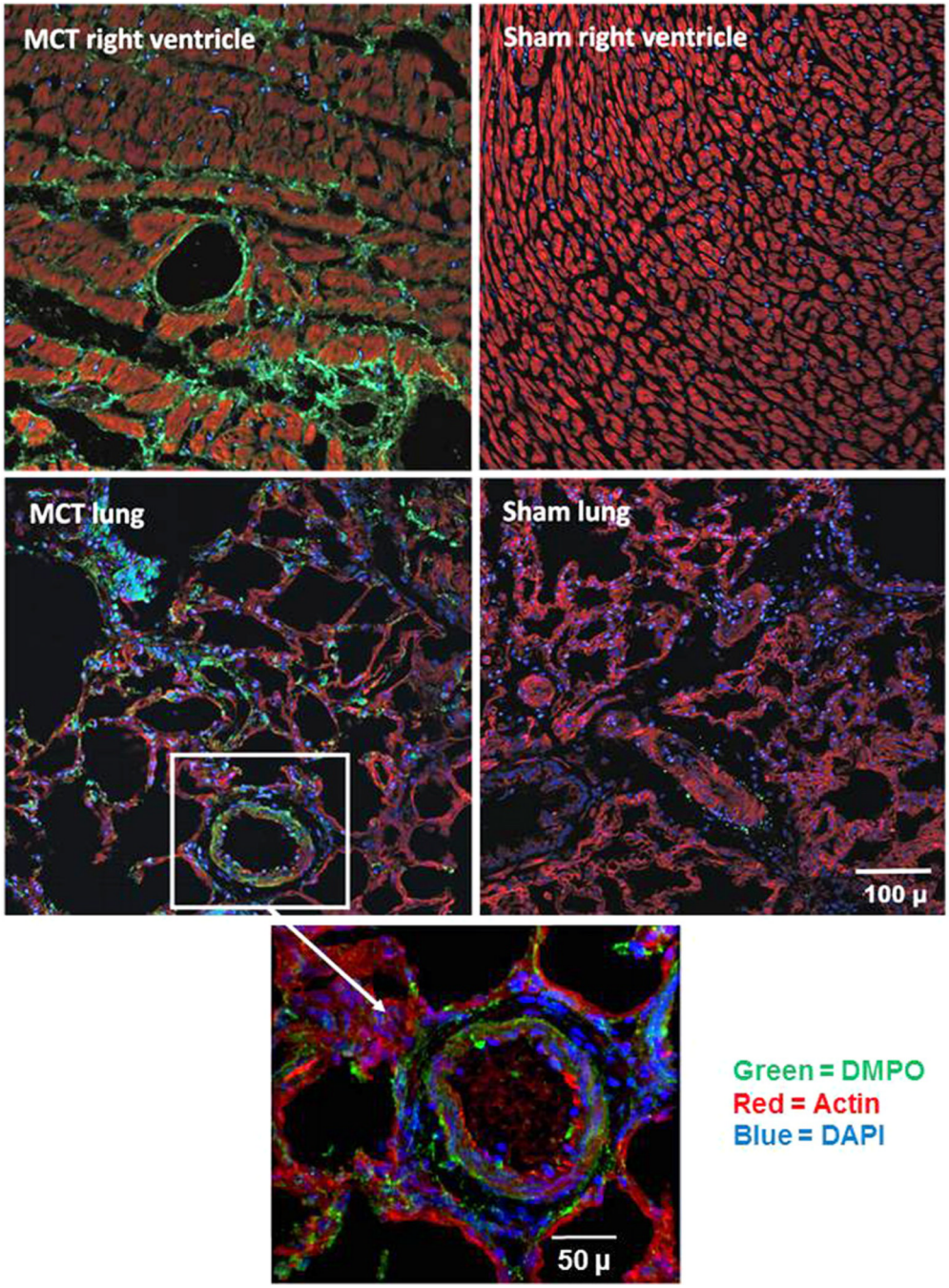

Fig. 5.

Monocrotaline-mediated free radical formation in rat lung and right ventricle. Three weeks after receiving monocrotaline (60 mg/kg ip) or saline (sham), rats received DMPO (2 g/kg total ip) in three doses 24, 12, and 6 h before sacrifice. At sacrifice, right ventricle (top) and lung tissue (bottom) were harvested, fixed, sectioned, and stained for DMPO–protein radicals using a primary rabbit polyclonal anti-DMPO Ab (green, DMPO; red, actin; and blue, DAPI nuclear stain). The white box and arrow indicate a magnified portion of the MCT-treated rat lung tissue. Data are representative images from three rats for MCT and three sham rats.